

See discussions, stats, and author profiles for this publication at: <https://www.researchgate.net/publication/315475641>

An agent-based model of avascular tumor growth: Immune response tendency to prevent cancer development

Article in SIMULATION: Transactions of The Society for Modeling and Simulation International · March 2017

DOI: 10.1177/0037549717699072

CITATIONS

35

READS

416

4 authors:



Fateme Pourhasanzade

University of Bergen

14 PUBLICATIONS 78 CITATIONS

[SEE PROFILE](#)



S.H Sabzpoushan

Iran University of Science and Technology

42 PUBLICATIONS 168 CITATIONS

[SEE PROFILE](#)



Ali Mohammad Alizadeh

Tehran University of Medical Sciences

19 PUBLICATIONS 297 CITATIONS

[SEE PROFILE](#)



E. Esmati

63 PUBLICATIONS 324 CITATIONS

[SEE PROFILE](#)



An agent-based model of avascular tumor growth: Immune response tendency to prevent cancer development

**Fateme Pourhasanzade^{1,4}, S.H Sabzpoushan¹,
Ali Mohammad Alizadeh² and Ebrahim Esmati³**

Abstract

Mathematical and computational models are of great help to study and predict phenomena associated with cancer growth and development. These models may lead to introduce new therapies or improve current treatments by discovering facts that may not be easily discovered in clinical experiments. Here, a new two-dimensional (2D) stochastic agent-based model is presented for the spatiotemporal study of avascular tumor growth based on the effect of the immune system. The simple decision-making rules of updating the states of each agent depend not only on its intrinsic properties but also on its environment. Tumor cells can interact with both normal and immune cells in their Moore neighborhood. The effect of hypoxia has been checked off by considering non-mutant proliferative tumor cells beside mutant ones. The recruitment of immune cells after facing a mass of tumor is also considered. Results of the simulations are presented before and after the appearance of immune cells in the studied tissue. The growth fraction and necrotic fraction are used as output parameters along with a 2D graphical growth presentation. Finally, the effect of input parameters on the output parameters generated by the model is discussed. The model is then validated by an *in vivo* study published in medical articles. The results show a multi-spherical tumor growth before the immune system strongly involved in competition with tumor cells. Besides, considering the immune system in the model shows more compatibility with biological facts. The effect of the microenvironment on the proliferation of cancer and immune cells is also studied.

Keywords

Agent-based model, tumor growth model, mathematical model, immune cell, recruitment, hypoxia

I. Introduction

Cancer research has received a surge of interest in recent decades. Computational or *in silico* modeling and the simulation of cancer growth and development play an important role in both experimental and clinical researches.¹ These models have become popular since they can prevent time-consuming and costly *in vivo* experiments.

Solid tumors are known to progress through three distinct phases of growth: the avascular phase, the vascular phase, and the metastatic phase.² In fact, a tumor always grows from a small number of malignant proliferative cells and goes through an initial avascular (without blood vessels) stage of growth. It has to develop its own blood supply to grow larger and more quickly. The process of inducing the formation of new blood vessels toward the tumor through secreting vessel chemoattractants by

starving cells is called angiogenesis.³ When a tumor is able to induce angiogenesis, it can become vascularized. Researchers often concentrate their efforts on each of these stages to answer specific questions. In this paper, we

¹Department of Biomedical Engineering, Research Laboratory of Biomedical Signals and Sensors, Iran University of Sciences and Technology (IUST), Iran

²Cancer Research Center, Tehran University of Medical Sciences, Iran

³Department of Radiation Oncology, Cancer Institute, Tehran University of Medical Sciences, Iran

⁴School of Electrical Engineering, Iran University of Science & Technology (IUST), Iran

Corresponding author:

Fateme Pourhasanzade, Iran University of Science and Technology, Electrical Engineering School, Tehran, 16846-13114, Iran.
Email: fateme.pourhasanzade@gmail.com

have focused on modeling the avascular tumor growth, that is, the tumor without any blood vessel.

Moreover, cancer is a complex disease⁴ that involves multi-spatiotemporal interaction at both molecular and cellular levels. The interactions between the tumor cells and their microenvironment⁵ that may lead to metastasis and tissue invasion, and also tumor-immune interactions during tumor progression, are examples of tumor complexity. Building models of complex biological processes needs an iterative procedure that considers relevant biological details.⁴ On the other hand, our understanding of tumor growth mechanisms is limited due to the extremely complex nature of the biological systems underlying the tumor behavior. Therefore, developing realistic models (mathematical, computational, or both) is a tough task.⁶

Complex biological systems and processes like cancer do not obey deterministic laws. With the same outputs and of comparable complexity, stochastic models can account for a larger part of the observed variation of model outputs than deterministic models. Mutations cannot deterministically be modeled in certain genes, since they are randomly occurring at discrete events. Besides, the natural history of cancer and its responses to therapy are stochastic processes.⁷ Hence, it is decided to use a stochastic model rather than a deterministic one in this study.

Regardless of being deterministic or stochastic, tumor growth models can be categorized into two general categories of continuous and discrete models, from a certain point of view. There is a third category called hybrid models, which combines the strengths of both discrete and continuous approaches. Continuous models are based on ordinary or partial differential equations (PDEs) and can describe the growth phenomenon. Ordinary differential equations (ODEs), used to study the growth of tumor cell populations, often lead to a conclusion of Gompertzian growth,⁸ which is given by Equation (1):

$$V = V_0 \exp\left(\frac{A}{B}[1 - \exp(-Bt)]\right) \quad (1)$$

where V_0 is the tumor volume at time $t = 0$, and A and B are constant parameters that can be fitted to comply with experimental data.⁹ However, real tumors always possess much more complex morphology. Besides, Gompertzian growth models are very limited since they cannot elucidate the underlying “microscopic” mechanisms of tumors.⁹ Moreover, they cannot simulate and predict the effect of chemicals on tumor morphology.

PDE models capture more complexity than ODE models. Using cell densities and nutrient concentrations as state variables, PDE models can be used to analyze various spatiotemporal phenomena.⁸ However, in some situations, individual and agent-based modeling (ABM) approaches, which treat cells as discrete objects with pre-defined rules of interaction, may offer an improvement

over differential equation methods.⁸ The ABM approach provides a natural description of a system as a form of computational science. ABM agents interact with and affect each other, consider individual decisions, learn from their experiences, and adapt their behaviors. Therefore, they are better suited to their environment. The ABM approach captures emergent phenomena. The whole system in emergent phenomena is truly greater than the sum of its parts, and because of the interactions between the parts, it cannot be reduced to its parts. Thus, the natural modularization follows boundaries among individuals, whereas it often crosses these boundaries in equation-based models. ABM is a flexible, easy to implement, low cost, and time-saving approach.¹⁰ However, the most important feature of ABM is its ability to deal with emergent phenomena.

In tumor growth modeling, it is important to characterize the model as simply and comprehensively as possible by considering the influence of necessary experimental or clinical details on tumor growth. Cancer progression involves events that occur at multiple time and spatial scales, the former ranging from seconds for microscopic cell interactions to months or years for macroscopic cell population level, and the latter ranging from the molecular level to the tissue level. Multi-scale models that link different spatial and temporal scales¹¹ have been widely applied in quantitative cancer researches over recent years.¹² The agent-based model that is proposed in the present study is one of the traditional methods in the multi-scale modeling of tumor growth.

The tumor growth described in this paper is restricted to the avascular stage where the cells receive nutrients and oxygen from existing blood vasculature. Avascular tumors can grow until the lack of nutrient and oxygen limits their development. One of the reasons to model avascular tumor growth is to develop and validate a foundational model in order to predict the behavior of the tumor in its early stages before tackling the more complicated vascularized stages of growth and metastatic behaviors. Besides, undetectable metastases after surgically removing the primary tumor can be modeled as early stage tumors. Therefore, it can be predicted whether the patient will need additional post-operative therapy.¹³ Moreover, we believe it is important to focus on avascular tumor growth before the more complicated vascularized stages of growth, since biologists and immunologists have a limited understanding of the interactions between individual tumor cells and tumor-immune cells.

The idea that the immune system could employ innate and adaptive immune responses to eliminate the microbial pathogens and aberrant cancer cells by scanning the body is not new.¹⁴ The tumor microenvironment consists of the innate immune (dendritic and natural killer) cells and adaptive ones (T and B lymphocytes).¹⁵ These diverse cells communicate with each other by means of direct

contact or cytokine and chemokine production, and act in autocrine and paracrine manners to control and shape tumor growth.¹⁵ The most frequently found immune cells within the tumor microenvironment are Tumor-associated Macrophages (TAMs) and T cells.¹⁶ As we mentioned, the immune system may help to fight cancer. For instance, cytotoxic T cells kill tumor cells by programming them to undergo apoptosis.¹⁷ Hence, this study concentrates on the searching process of immune cells for tumor cells, and the tumor-immune cell interactions.

1.1 Review of previous models

Over the past decades, scientists have shown significant interest in the mathematical modeling of tumor growth and the dynamics of the immune system.¹³ Since biochemical activities have been often observed in biological systems (for example, the metabolic activity necessary for cellular growth and survival), biological systems can be modeled as systems with a set of chemical reaction processes. Therefore, the mathematical analysis used in the development of chemistry can be applied as a powerful tool in biological models.⁴

One of the first attempts to achieve a model of solid tumor growth was a simple model proposed by Burton¹⁸ introducing the diffusion and nutrient concentration limit on tumor growth. Since then, different models including lots of large systems of differential equations have been suggested based on their special goal of modeling and the amount of detail used. An innovative model presented by Kansal et al.¹⁹ in 2000 using cellular automata to express the growth of Glioblastoma multiforme (GBM)—the most malignant brain tumor—was another important effort in the modeling of tumor growth, which was later developed by Torquato.⁹ This avascular tumor growth has shown that macroscopic tumor behavior can be affected by microscopic parameters.

Another valuable attempt in modeling cancer growth was reported by Abbott.²⁰ CancerSim, a three-dimensional agent-based model, implemented tumor growth simulation from the perspective of intracellular dynamics based on Hanahan and Weinberg's²¹ hallmarks of cancer (representing the failures needed within a cell to become a cancerous cell).

Mathematical and computational models of avascular tumor growth,^{2,22} angiogenesis,^{23,24} vascular tumor growth,²⁵ invasion,^{22,26} the effect of microenvironmental factors on tumor growth,^{27,28} and treatment²⁹ have been reviewed from many aspects and viewpoints. In addition, a brief review of mathematical models, including a history of each of model, can be found in an article written by Araujo and McElwain.³⁰ Moreover, Byrne et al.,³¹ Chaplain,³² Hatzikirou et al.,³³ Materi,⁴ and Rejniak and Anderson³⁴ separately reviewed mathematical and computational models of tumor growth or invasion.

Merrill³⁵ described the kinetics of the cellular immune response mathematically. There are also a number of models studying the interaction between the immune system and tumor growth. An overview of these models can be found in Eikenberry et al.'s paper.³⁶ Most of these models are deterministic, and comprised of ODEs³⁷ or PDEs.³⁸ A comprehensive review of the tumor-immune system models is given by Adam and Bellomo³⁹ and Wilkie.⁴⁰ A brief review of non-spatial mathematical models of tumor growth-immune system interaction was recently studied by Eftimie⁴¹ as well.

Olsen and Siegelmann⁴² proposed a new discrete agent-based approach to model tumor angiogenesis. However, the strategy we employed to describe the tumor growth is quite different. Considering the role of the immune system in tumor growth progression and in the fight against tumor cells, our proposed model simply includes cellular and tissue levels of representation, while Olsen and Siegelmann's model includes cellular, tissue, and molecular levels. Our model is also different from the hybrid cellular automata-PDE approach, another technique that can be used in such research, which was employed by Mallet and De Pillis¹³ to describe tumor-immune system interaction next to a nutrient source by using biological cell metabolism rules.

None of the above models consider how the microenvironment affects the proliferation of cancer cells, and how cancer cells affect the rest of the system, especially in the recruitment of immune cells. However, we have considered the effect of the microenvironment on the proliferation of tumor cells and the recruitment of immune cells by using a spatial representation of cells, as it is more similar to the original biological system. Moreover, unlike the other spatiotemporal models mentioned above, our proposed model allows the consideration of individual cell behavior and associated randomness, rather than applying a general rule to a collection of cells.

2. Method

The proposed model is based on four fundamental properties: biological concepts and assumptions, physical structure, various modes, and updating rules.

2.1 Biological concept

In this study, it is assumed that the tumor growth process starts from a small number of abnormal cells⁴³ and continues to grow as a multicellular spheroid (MTS). In a MTS structure, as the tumor grows, it becomes more difficult for the core or center of the spheroid to reach the nutrients, since the outer cells tend to consume these nutrients first.^{9,19} Therefore, cells close to the core (middle layer cells) can become so deficient that they lose their ability to be proliferating and enter the quiescent stage. Quiescent (non-proliferative) cells are still alive, and can be

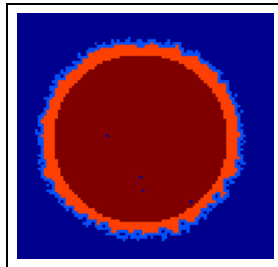


Figure 1. The three layers of the spherical structure of a solid tumor growth. The light-blue (medium gray) outer region is comprised of proliferating cells, the light-red (light gray) region is non-proliferative cells, and the dark-red (dark gray) region is necrotic cells.

Table I. Summary of the two agents and their possible modes.

Agent	Brief description	Modes
NIC	Non-immune cells	Normal cells (N) Proliferative cancer cells (PT) Non-proliferative cancer cells (NT) Necrotic cells (Ne)
IC	Immune cells	Natural killer cells (NK) Cytotoxic T lymphocyte cells (CTL)

recovered with accessing sufficient nutrients.¹⁹ In addition, the inner core is formed as a mass of dead cells that do not digest and dissolve, known as a necrotic core due to insufficient nutrients. Eventually, the outer core consists of active tumor cells (proliferating).¹⁹ Only this type of tumor cell has the capability to replicate and participate in mitosis. Therefore, a typical MTS (Figure 1) consists of an outer shell of proliferating cells, an inner layer of quiescent cells that are dormant but viable, and a central core of necrotic material.¹⁹ It should be mentioned that consistent colors are used in the results. Proliferating tumor cells, non-proliferating tumor cells, necrotic entities, and normal cells are depicted in light-blue (medium gray), light-red (light gray), dark-red (dark gray), and dark-blue (black), respectively.

2.2 Physical structure and various states

The proposed model is a two-dimensional (2D; n -cell \times n -cell) square network, filled with two types of agents: immune or non-immune cells placed at the (i,j) coordinate system where $0 < i,j < n$ -cell. The agents have some possible modes, which are tabulated in Table 1.

1. Agent NIC (Non-immune Cells) can have four modes: 0—normal (N); 1—proliferative cancer

(PT); 2—non-proliferative cancer (NT); 3—necrotic (Ne). Besides, empty places in the studied tissue are shown by agent NIC in mode 0. This agent can proliferate and affect its neighboring cells in mode 1.

2. Agent IC (Immune killer Cells or I-cells), including Natural Killer (NK) cells and Cytotoxic T Lymphocyte (CTL) cells, has two modes: 0—NK cells, which are supposed to die immediately after a collision with cancer cells; and 1—CTL cells, which are supposed to die after the maximum n -times, where n is a random number.

CTL and NK cells have the same functions. However, the main difference between them is that CTL cells identify specific antigens, while NK cells are major components of the innate immune response to the disease and they often lack antigen-specific cell surface receptors. Agent IC can move randomly in the tissue, by substituting for agent NIC in state 0. In addition, they can recruit new agent IC as a function of the number of successes in defeating agent NIC in state 1, that is, the future number of newborn agent IC depends on the ability of agent NIC in killing PT cells from the current iteration.

The model includes two sets of updating rules in cellular level of biological system: two sets of the transition rules for an agent in one group of agents (either agent IC or agent NIC), and a set of the decision mechanisms of the interactions between different types of agents. It should be noted that a group is a collection of agents of the same type. In other words, the agents' actions and interactions can be classified into the immune cells' movements toward tumor cells, mitosis of PT cells, and competition between populations of cells including healthy, tumor, and immune cells. In addition, two types of interactions, namely the interactions between tumor cells and normal cells, and the interactions between tumor-immune cells are considered in this model.

The transition rules of this model are probabilistic. Moreover, nutrient distribution is supposed to be uniformly distributed in the lattice. The nutrient deficiency is considered by the lack of free space within a certain distance of a cell. Therefore, a PT cell (agent NIC in mode 1) can only divide with related probabilities (Equation (2)) into two daughter cells where there is an empty space within a specific distance of it to put its second daughter cell, while the first daughter cell will replace its parents' position.

2.3 Updating rules

2.3.1 Rules related to agent NIC. Internal interaction between different types of cells in agent NIC leads to introducing the tumor growth and evolution rules. These rules will change the mode of the agent, and the competition between normal cells and proliferating tumor cells for nutrients, which is shown by free spaces in the lattice.

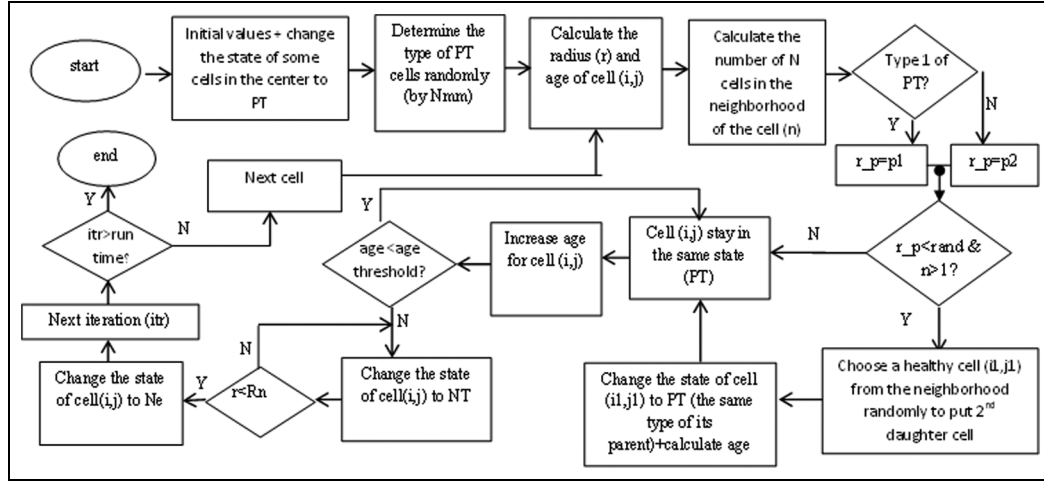


Figure 2. State transition rules of the components of agent NIC.

Each agent NIC in mode 1 (PT cell) can proliferate with probability r_p as a function of time and space. Here, we suppose two types of PT cells. Type 1 (mutant PT cell) does not consider the impact of the microenvironment on tumor growth, while the division of type 2 (non-mutant PT cell) is a function of the number of agent NICs in mode 0 (normal cells) surrounding the PT cell. Therefore, when there are more healthy cells around a non-mutant PT cell, the probability of division of that PT cell is greater due to accessing sufficient nutrients or oxygen. Non-mutant PT cells can help us consider a well-known phenomenon, such as hypoxia, in the tissue. In fact, the smaller the number of any type of PT cells around a non-mutant PT cell, the less oxygen is consumed and therefore the more probable it is that the cell proliferates:

$$r_p = \begin{cases} p_1; & \text{type1 of PT cell} \\ p_2; & \text{type 2 of PT cell} \end{cases} \quad (2)$$

An additional parameter of maximum external radius (R_{\max}) is introduced to assure that the results of the model fit the Gompertz curve. Therefore, the dynamics of the model is considered such that the division probability in the radii greater than R_{\max} is zero. This shows the dynamic pressure effects of the environment on the tumor growth. Thus, the tumor growth will stop in this radius due to the lack of nutrients.^{9,19} The probabilities p_1 and p_2 can be expressed by Equation (3):

$$\begin{aligned} p_1 &= p_0 \left(1 - \frac{r}{R_{\max}}\right), \\ p_2 &= \varphi_0 \times (\text{Number of } N \text{ cells in the neighborhood}) \\ &\quad \times \left(1 - \frac{r}{R_{\max}}\right) \end{aligned} \quad (3)$$

where p_0 and φ_0 are the base probabilities of the division of mutant and non-mutant PT cells, respectively, and r reflects the distance of each dividing cell from the center of the lattice.

At each time step, if the mode of an agent NIC is 1 (a PT cell of any type), the agent is checked to see if it can be divided. In this case, there should be an empty place. If there is at least one agent NIC in mode 0 in its neighborhood, the PT cell will choose that agent with the probability r_1 and then it will divide. Thus, one of the daughter cells will remain in the same position as the parent. The other daughter will place in that empty or normal neighbor, and the mode of that agent (NIC in mode 0) will change to 1. If the PT cell cannot find any agent NIC in mode 0 (an empty place or a normal cell) in its neighborhood to put the second daughter cell in or if it cannot proliferate with probability r_p within a specific distance (δ_p , i.e., the thickness of PT cells) from the tumor's edge, it would stay as a PT cell up to a certain time (as a function of the number of time steps). Therefore, each PT cell has an age counter that is incremented at every time step. After a mitosis, the age counter of daughter cells reset to zero. Besides, after reaching a certain time, named “age threshold,” of the PT cell, the PT cell can change to an NT cell, which is an unstable and intermediate state. In other words, the mode of the agent NIC will change from 1 to 2. The PT cell will turn to an NT cell when it is at a distance greater than δ_p , which is a certain distance from the tumor's edge.

The NT cell (mode 2) will then turn to a necrotic cell (mode 3) at a distance greater than $\delta_n + \delta_p$ from the tumor's edge due to the lack of nutrition in the next time step. However, if the NT cell is within a specific distance δ_p of the average tumor radius, it will turn to a PT cell (mode 1) due to accessing sufficient nutrient.

The Ne cells accumulate in the inner part of the tumor and are formed as a mass of dead cells. The mode of Ne cells will never change to any other modes. Besides, they will not dissolve following their encounter with an agent IC (immune cell).

Considering the assumption that as the tumor grows, it will shape as a multi-cell spheroid, the radius of the necrotic region (R_n) and the value of the thickness of PT cells (δ_p) are obtained using Equation (4)^{9,19}:

$$R_n = R_t - (\delta_n + \delta_p); \delta_n = aR_t^{2/3} \text{ & } \delta_p = bR_t^{2/3} \quad (4)$$

where a and b are constant parameters that reflect nutritional needs for tumor growth. R_n is a function of the time step and R_t is the average tumor radius calculated by obtaining the external edge of the tumor.

In summary, the mode of an agent NIC is eventually checked. The mentioned rules are followed in any mode rather than 0. In mode 1, a PT cell can divide with probability r_p regardless of its type. Therefore, the randomly chosen healthy cell (mode 0) will change to a newborn PT cell in the Moore neighborhood of that PT cell. Besides, the primary PT cell will preserve its mode. Otherwise, it will change to an NT cell (mode 2) after a number of time steps. If the distance of an NT cell is greater than $\delta_n + \delta_p$ from the tumor's edge, the mode will turn to a necrotic cell due to the lack of nutrition. Hence, the mode of the agent NIC will change to 3. Figure 2 shows a flowchart of changing the modes of components of the agent NIC.

2.3.2 Rules related to agent IC. In order to discuss the interactions between two agents (tumor-immune interactions), it is supposed that tumor cells release signals¹³ that can be detected by immune cells via specific receptors. Then, the immune cells move toward the center of the tumor because we have assumed that debris from dead tumor cells may help the immune system recognize its target. In this study, the movement of immune cells toward the tumor (the average density of the tumor in the studied tissue per volume) is modeled. For greater simplicity, the process of propagation of the released signal by the tumor cells and its receipt by immune cells is ignored. Thus, we hypothesized that the immune cells enter from one corner of the lattice to the studied tissue. These cells can freely move to the center of the tumor with probability r_walk , which is obtained from Equation (5):

$$r_walk = k \times [(nT/n_{cell}^2), (nPT/nT)] \quad (5)$$

where k is a damping constant considered as the ratio of the number of immune cells to the total number of cells in the lattice. nT , n_{cell}^2 , and nPT are the total number of tumor cells, total number of cells in the lattice, and the total number of PT cells, respectively.

The advantage of the possibility of immune cells walking in Equation (5) is that this type of initial biased random walk followed by an unbiased random walk increases the speed of movement of immune cells at the start of tumor growth where tumor cells are more proliferative than necrotic, that is, the ratio nPT/nT is obviously greater than the ratio nT/n_{cell}^2 . Once the immune cells are close enough to the PT cells, they can move randomly (unbiased random walk) in any direction to fight with tumor cells. Since the tumor grows quickly, some cells do not get enough nutrients and become necrotic. Therefore, in this case, the ratio nT/n_{cell}^2 plays a fundamental role in the random movement of immune cells.

When an agent IC meets an agent NIC in mode 1 (a PT cell), one of the following situations will happen.

1. Anti-tumor state: a PT cell may die because of cytotoxic T cells (CTLs) with probability r_I (Equation (6)) and its state (mode) will change to an unstable state. Then, this unstable state will change to 0. Here, $K0$ is the tumor death constant while $nI1$ and $nPT1$ are the numbers of immune and tumor cells in the neighborhood of the related cell. In other words, the agent IC will replace agent NIC in mode 1 with probability $K0$, while agent NIC disappears. If there is more than one agent NIC in the nearest neighborhood of agent IC in mode 1 (CTL), the same procedure will happen for each of the PT cells, and agent IC in mode 1 will replace one of them randomly. However, if the mode of agent IC is 0, one PT cell will be first chosen randomly and the transition rule will apply to it:

$$r_I = K0 * (nI1)/nPT1 \quad (6)$$

2. Neutral state: the PT cell will survive and remain in its previous state. The immune cell in any state will continue its search to find another PT cell.
3. Pro-tumor state: immune cells will fail in killing PT cells and die with probability r_t (Equation (7)). In this case, the cancer cell will survive and the immune cell will switch to become an empty space or N cell, that is, the mode of agent NIC will stay the same. However, agent IC will disappear and an agent NIC in mode 0 will be born and replace it. Here, $K1$ is the immune death constant. $nI1$ and $nPT1$ are mentioned before in Equation (6):

$$r_t = K1 * nPT1/nI1 \quad (7)$$

If agent IC does not find a PT cell in its Moore neighborhood, it will continue walking randomly. Therefore, it will search for either an N cell or an empty space in its Moore

Table 2. Summary of time-dependent functions and input parameters for the proposed model.

Parameters	Brief explanation	Parameters	Brief explanation
nT	Total number of tumor cells in the tissue	r_p	Probability of PT division (varies with time and position)
nPT	Total number of PT cells in the tissue	r_{walk}	Probability of immune cell walking randomly
	Number of PT cells in the neighborhood of a site	r_t	Protumor probability
nII	Number of immune cells in the neighborhood of a site	r_I	Antitumor probability
R_t	Average overall tumor radius	δ_p	Proliferative rim thickness (determines growth fraction)
R_n	Average overall necrotic layer radius	δ_n	Non-proliferative thickness (determines necrotic fraction)
Nmm	Initial probability of ratio of non-mutant cells to mutant cells		

Table 3. Input parameters and their initial values used in the proposed model.

Parameter	Brief explanation	Value
p_0	Base probability of division of mutant PT cell	0.7
φ_0	Base probability of division of non-mutant PT cell	0.06
a	Base necrotic thickness, controlled by nutritional needs	0.42
b	Base proliferative thickness, controlled by nutritional needs	0.11
R_{\max}	Maximum tumor extent, controlled by pressure response	37.5
K_0	Tumor death constant	0.5
K_I	Immune death constant	0.2

neighborhood to move for the next iteration. Otherwise, agent IC will remain in its previous position.

In the proposed model, the ability to recruit immune cells is considered as a function of successes and failures in the killing of tumor cells (Equation (8)), which means the direct internal interaction between two different types of agents:

The number of newborn immune cells =

$$(v - f) \times nPT/nT \quad (8)$$

where v and f are the numbers of successes and failures in killing tumor cells, respectively. If the number of newborn immune cells is positive, the recruitment of immune cells will happen. Therefore, some random empty places (agents NIC in mode 0) will be searched and replaced by immune cells. The number of cells searching for these empty places is the same as the number of newborn immune cells in Equation (8).

It is important to note that we implement short distance or contact-dependent (cells will only signal other cells they have physical contact with) communication as the biological communication system in this model.

3. Simulation design

Firstly, consider a 2D ($L \times L$) tissue composed of two agents with their special different modes denoted by NIC

and IC. Figure 3 shows a block diagram of the connection of these agents in the tissue and cellular levels in general. This figure shows although both agents NIC and IC are considered separately in the tissue level, they are not separated at the cellular level. In fact, the entire tissue is covered with healthy cells of agent NIC, which means agent NIC is in state 0. In addition, a few numbers of agents IC are deployed in a corner of the lattice.

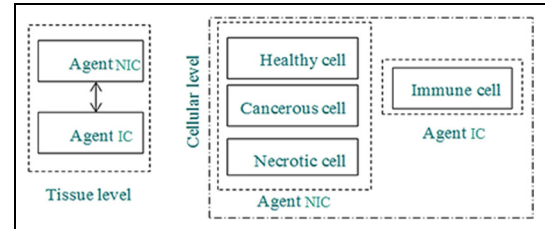


Figure 3. Agents NIC and IC in the cellular and tissue levels. Here, we depicted modes 1 and 2 of agent NIC by a single box labeled “cancerous cell.”

Then, a few cells within a fixed initial radius of the center of the lattice are designated proliferative. Therefore, their state will change from 0 to 1 in agent NIC. Tables 2 and 3, respectively, show the variables and parameters used in the model, with their initial values.

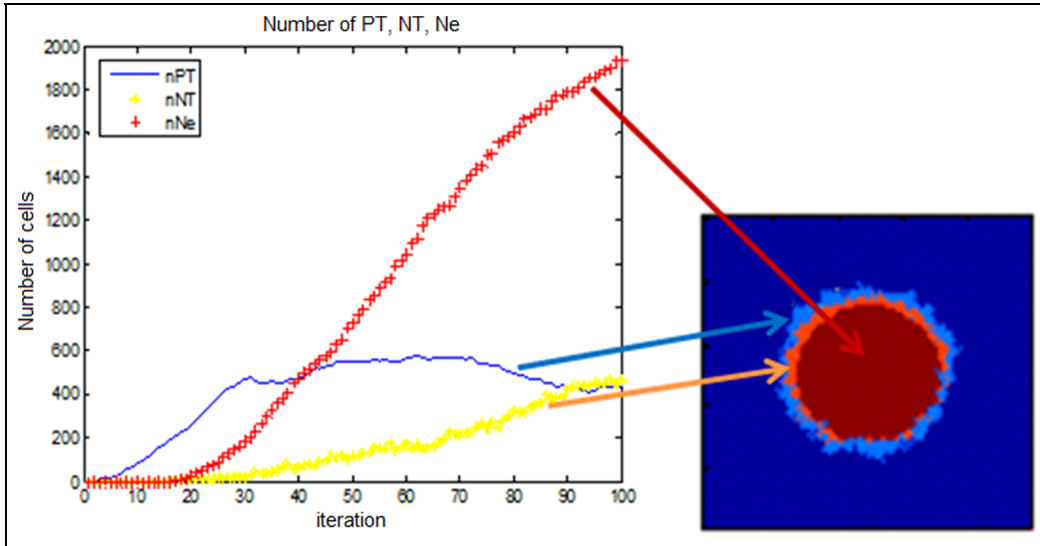


Figure 4. The numbers of cell types of agent NIC without considering any interaction with agent IC and a snapshot of simulated tumor growth without any immune cell. The light-blue (medium gray) region, light-red (light gray) region, and dark-red (dark gray) region are comprised of proliferating tumor cells, non-proliferative tumor cells, and necrotic cells, respectively. The scales are in millimeters.

The internal interactions of a single agent model are considered for studying the presence or absence of agent IC (the immune system). The results, discussed in the next section, have been reported assuming $a = 0.42$, $b = 0.11$, and $R_{\max} = 37.5$, where R_{\max} is the maximum radius of a brain tumor and is extracted from the articles by Torquato⁹ and Kansal.¹⁹ Parameters a and b are chosen to fit the tumor growth procedure in the terms of quality.^{9,19} In addition, periodic boundary conditions are implemented for the random walks of the cells.

4. Results

Firstly, the results of a single agent model (agent NIC) and the effect of input parameters on the output parameters generated by the proposed model are reported. The numbers of different modes of agent NIC containing proliferating, non-proliferating, and necrotic cells in 100 time iterations and before the immune system even starts to recognize cancer cells is shown in Figure 4. As can be seen, due to the lack of nutrients (shown by the lack of free space in the neighborhood in the proposed model) in an avascular tumor, the number of necrotic cells will increase aggressively and reach 1900 cells during simulation. Meanwhile, the number of PT cells that have exponentially increased at an early stage of cancer development will decrease and reach a limit of 450 cells. Intuitively, Figure 4 shows that PT cells follow Gompertzian growth dynamics. Central cross-sections of the tumor are considered as outputs of our simulations to show the spatial distribution of tumor growth over time.

Figure 5 shows the changes in the average radius of the external edge of the tumor, the radius of the necrotic core, growth fraction, and the necrotic fraction in each iteration. The growth fraction is the ratio of the number of proliferative cells to the number of whole tumor, cells while the necrotic fraction is the ratio of the number of necrotic cells to the number of whole tumorous cells. This figure provides supporting evidence that shows growth-limitation due to a lack of nutrients in avascular tumor. As can be seen, because of the loss of nutrients, the growth fraction decreases to 0 and the necrotic fraction increases to 0.9.

Figure 6 shows the rate of change of different types of agent NIC in mode 1: mutant and non-mutant proliferating tumor cells. It should be mentioned that at the beginning, we considered 20% of our PT cells as non-mutant ones (i.e., $N_{mm} = 0.2$). As the figure depicts, the number of mutant PT cells almost linearly increases since these PT cells precede mitosis without considering the effects of the tumor micro-environment. However, the number of non-mutant PT cells tends to increase through Gompertz growth dynamic and reaches 11.5% of the number of total PT cells. Due to the influence of the tumor microenvironment on the non-mutant PT cells, the smaller the number of empty spaces in the neighborhood of a parent cell, the less proliferation happens.

Figure 7 shows the changes of different modes of agent NIC (all types of PT cells, NT and Ne cells) against N_{mm} . Moreover, Figure 8 depicts the effect of N_{mm} on the growth and necrotic fraction. As can be seen, the changes in N_{mm} value do not show any significant difference in the appearance of the figures, while there are no immune cells in the studied tissue.

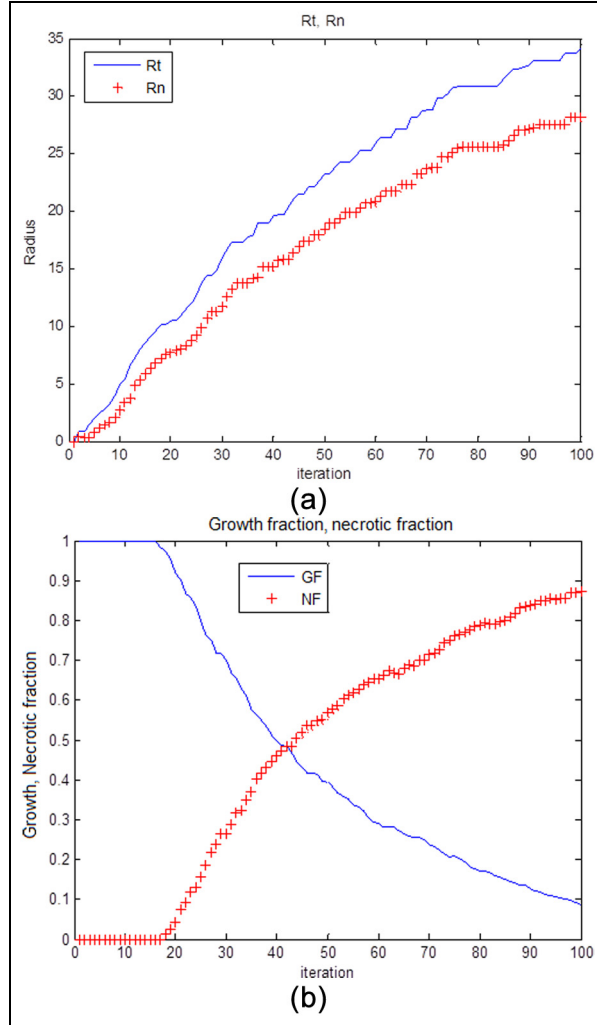


Figure 5. (a) The rate of change of the average radius of R_t . (b) The rate of change of the growth and necrotic fractions in a 100-iterations run.

Figure 9 shows the effect of changing N_{mm} values on the ratio of mutant PT cells to non-mutant PT cells in each iteration. It can be seen that this ratio will initially rise over time and then, at the end of the simulation, it will reach the mean value of 9 as a saturation value. In addition, regardless of the different initial probability values of this ratio, the temporal ratio changes will approximately follow the same dynamic.

In the following, parts of the results of the existence of immune cells next to the agent NIC are reported. Figure 10 represents the entrance and movement of agent IC (immune cells) toward the tumor, the interaction between two agents NIC and IC (i.e., immune cells and tumor cells), and immune cell recruitment as the tumor grows. It shows the nonlinear increase in the number of immune cells in the studied tissue due to their triumph of killing tumor cells.

Figure 11 shows the number of different modes of agent NIC (proliferating tumor cells, non-proliferating tumor cells,

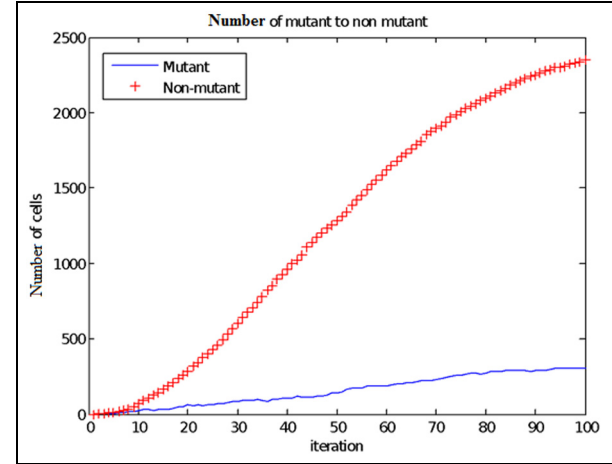


Figure 6. The rate of change of the mutant and non-mutant PT cells before the presence of immune system. $N_{mm} = 0.2$.

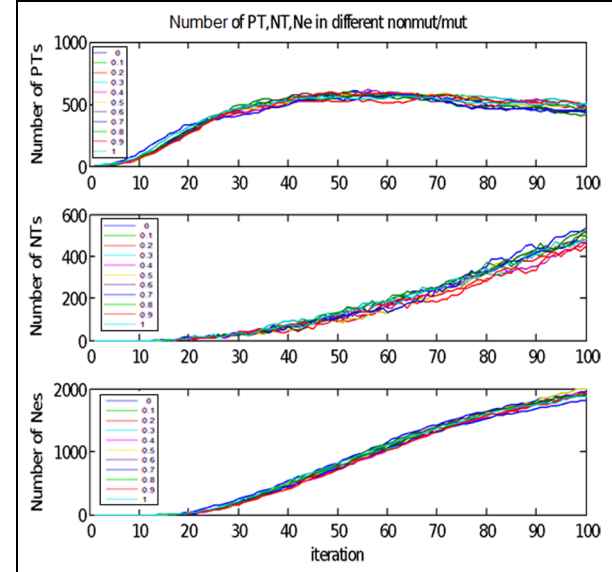


Figure 7. The effect of changes of N_{mm} on the changes of the number of diverse cell types.

necrotic cells), and the number of agent IC (immune cells) during the simulation when $N_{mm} = 0.9$. It is obvious from this figure that the number of immune cells is enhanced due to recruitment. In fact, the immune cells and the process of their recruitment are modeled to destroy a mass of tumor as an anti-tumor mode rather than helping grow the mass. The total tumor cells occupy 25% of the tissue, while it was 28% in the absence of agent IC, which shows a 89% decrease in the size of the tumor in the presence of immune cells.

Figure 12 depicts the effect of changing the values of N_{mm} from 0 to 1 in 0.1 increments. As expected, the agent IC that arrives at the system with some delay leads to a reduction of the number of PT cells compared to Figure 7.

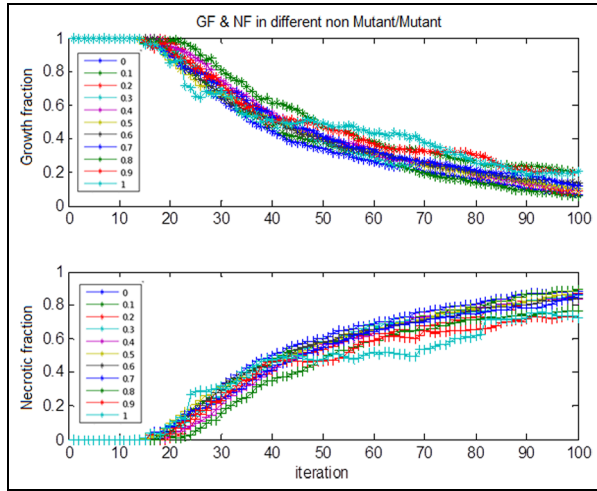


Figure 8. The effect of changes of N_{mm} on the changes of growth and necrotic fractions before the presence of the immune system.

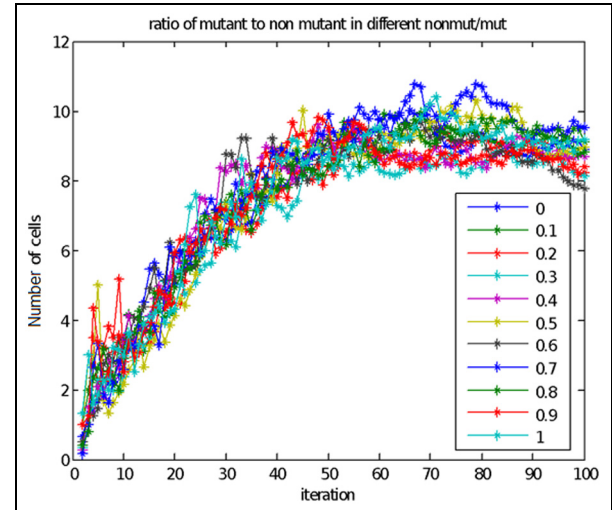


Figure 9. The effect of changes of N_{mm} on the changes of the ratio of mutant PT cells to non-mutant PT cells before the presence of the immune system.

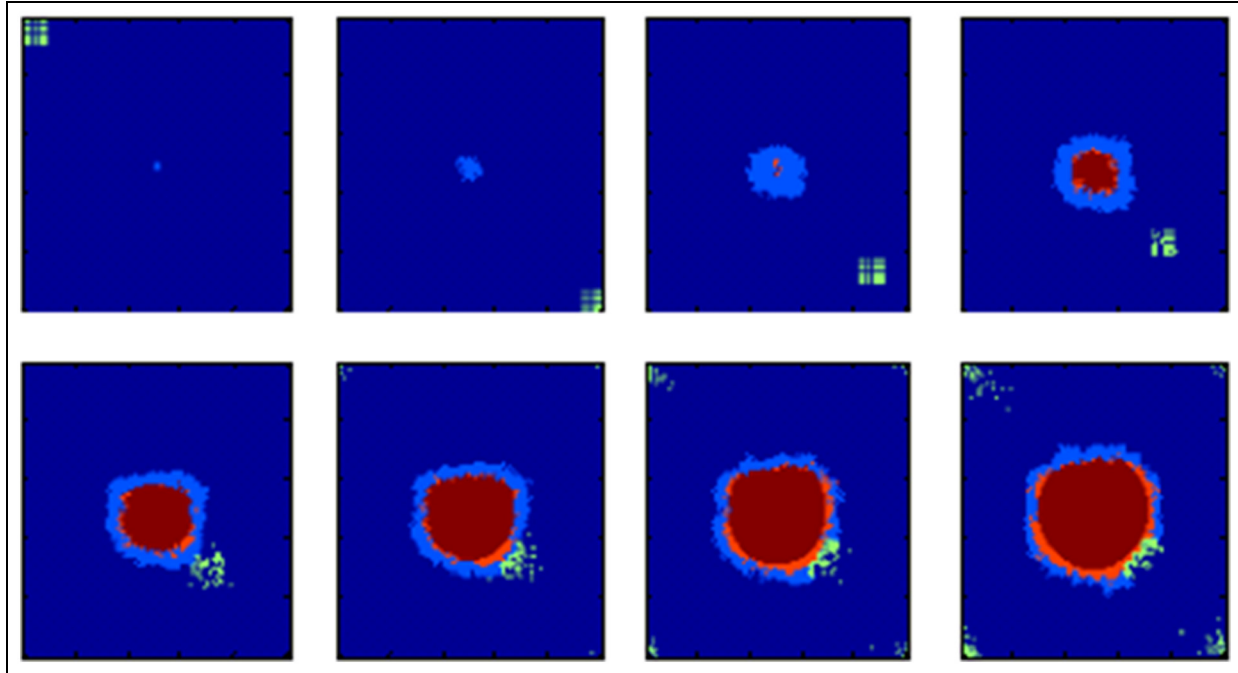


Figure 10. The influx of agent IC from a corner of the lattice and interaction with agent NIC and immune cell recruitment at simulation time $t = 1, 10, 20, 30, 40, 50, 60$, and 80 . The outer light-blue (medium gray) region, the light-red (light-gray) region, and the dark-red (dark-gray) region comprise proliferating tumor cells, non-proliferative tumor cells, and necrotic cells, respectively. The yellow (white) dots are immune cells. The scales are in millimeters.

It is also observed that the slopes of the last curves and the final values of the number of immune cells can change by varying the value of the N_{mm} -parameter. This shows how the microenvironment affects the proliferation of cancer cells and how these cancer cells affect the rest of the system, especially the number of immune cells. However,

there are no significant changes in the number of other types of cells when varying this parameter.

The rate of change of the average radius of the tumor and necrotic core, the growth fraction, and necrotic fraction are shown in Figure 13. It can be seen that the tumor growth stops in a radius less than the maximum tumor

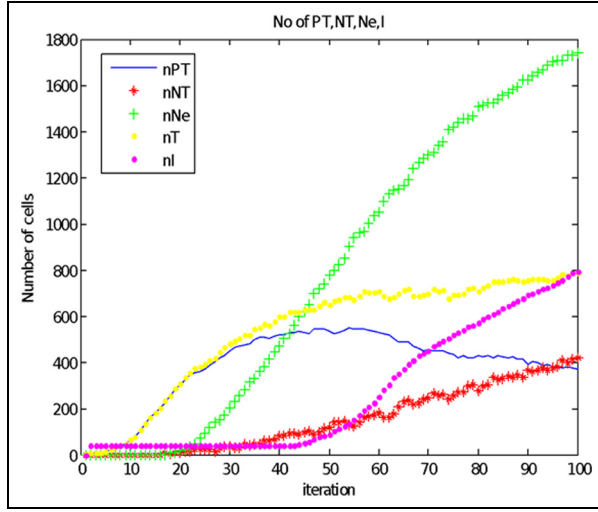


Figure 11. The number of PT, NT, Ne, and I cells at each iteration time when $Nmm = 0.9$. The total number of PT and NT cells is shown by nT in this figure.

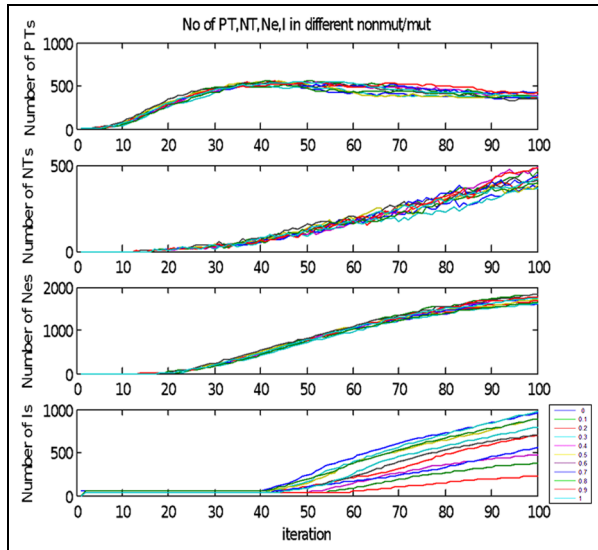


Figure 12. The effect of changes of Nmm on the changes of the number of PT, NT, Ne, and I cells.

extent (R_{\max}). In addition, the presence of the immune system in the tissue leads to a decrease in changing the state of agent NIC from PT cells to NT cells and eventually NT to Ne cells by killing the PT cells. Therefore, in this case, it will affect the necrotic fraction to 0.7 but there is no significant change in the ultimate value of the growth fraction. However, reducing the growth fraction after the arrival of the immune system begins a little earlier than the situation in which the immune system is not considered in the model.

Figure 14 shows the variation of the ratio of mutant PT cells to non-mutant PT cells due to the changes of Nmm

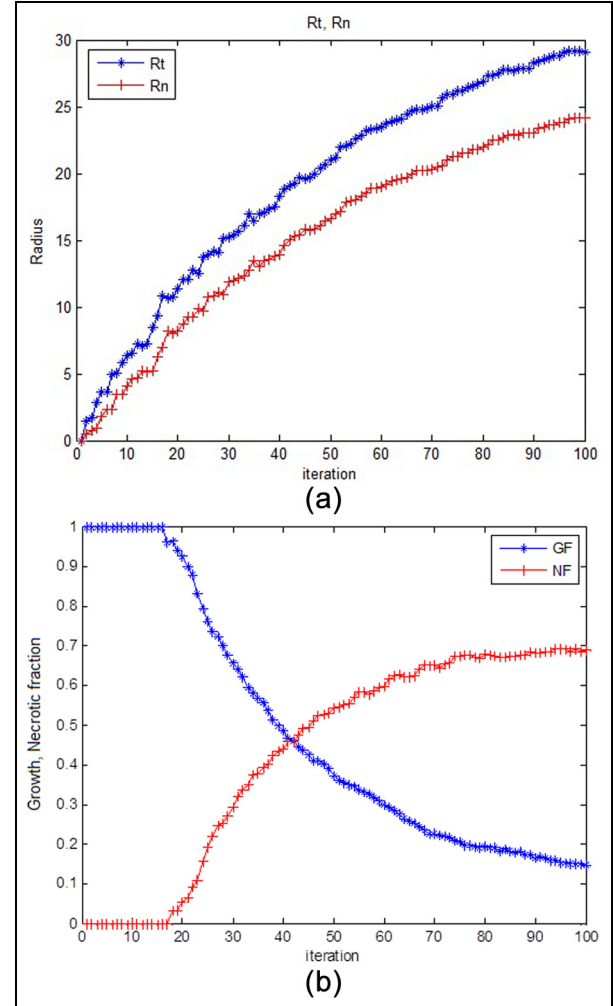


Figure 13. (a) The rate of change of the average radius of R_t and R_n . (b) The rate of change of the growth and necrotic fractions in a 100-iteration run after the influx of immune cells.

after entering the immune cells. There is no certain change observed compared to the results of Figure 9. The only difference is in the average saturation value, which increases to 13. In other words, after adding agent IC to the model and considering its effects, the ratio of mutant PT cells to non-mutant PT cells is 1.44 times higher than the results reported for simulating a single agent model. Besides, the increasing slope of the variation of the ratio of mutant PT cells to non-mutant PT cells in this figure is more than that in Figure 9.

The effect of different Nmm on the number of various types of cells, the radii of the tumor and necrotic core, the growth fraction and necrotic fraction, and the ratio of non-mutant PT cells to mutant PT cells at two arbitrary simulation times, 20 and 50, are shown in Figure 15. It can be seen that changes in Nmm lead to changes in the number of PT and NT cells in both simulation times. Small changes in the number of immune cells are also seen at $t = 50$. It

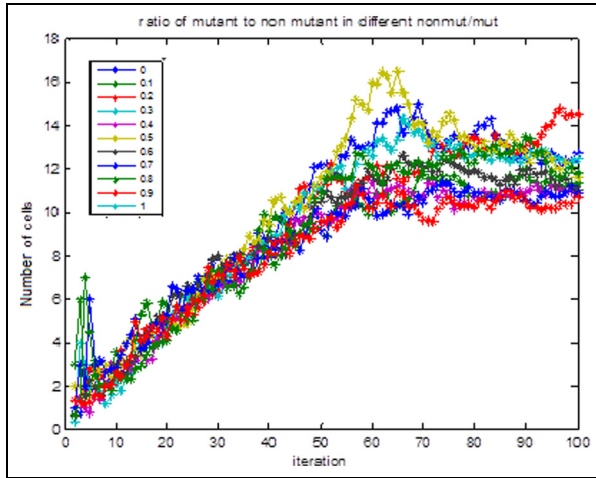


Figure 14. The variation of the ratio of mutant PT cells to non-mutant PT cells by changing N_{mm} after the influx of the immune system.

seems that the radii of the tumor and necrotic core are affected by the changes of N_{mm} . However, the growth and necrotic fractions are not dependent on the changes of this parameter. Eventually, as expected, the ratio of non-mutant

PT cells to mutant PT cells is strongly influenced by N_{mm} variations.

Figure 16 shows the effects of the tumor death constant due to the immune system (K_0), while Figure 17 represents the effect of the immune cells death constant due to the immune system (K_1). As expected, a significant difference in the number of immune cells can be seen in these two figures. In Figure 16, the maximum of K_0 shows the maximum number of immune cells during simulation. However, the maximum of K_1 leads to the complete destruction of immune cells. Therefore, the increase of K_1 will decrease the anti-tumor behavior of the immune system. In this case, the recruitment process will not occur, since this process is directly related to the success in killing tumor cells.

Figure 18 shows the entrance and movement of agent IC toward the tumor, and the interaction between two agents NIC and IC, that is, immune cells and tumor cells when $N_{mm} = 0.2$. This shows how the microenvironment affects the proliferation of cancer cells, and how these cancer cells affect the rest of the system, especially the amount of recruitment of immune cells. Comparing this figure with Figure 10 represents the effect of N_{mm} , which shows the indirect effect of the microenvironment on the number of immune cells entering the studied tissue. It also affects the

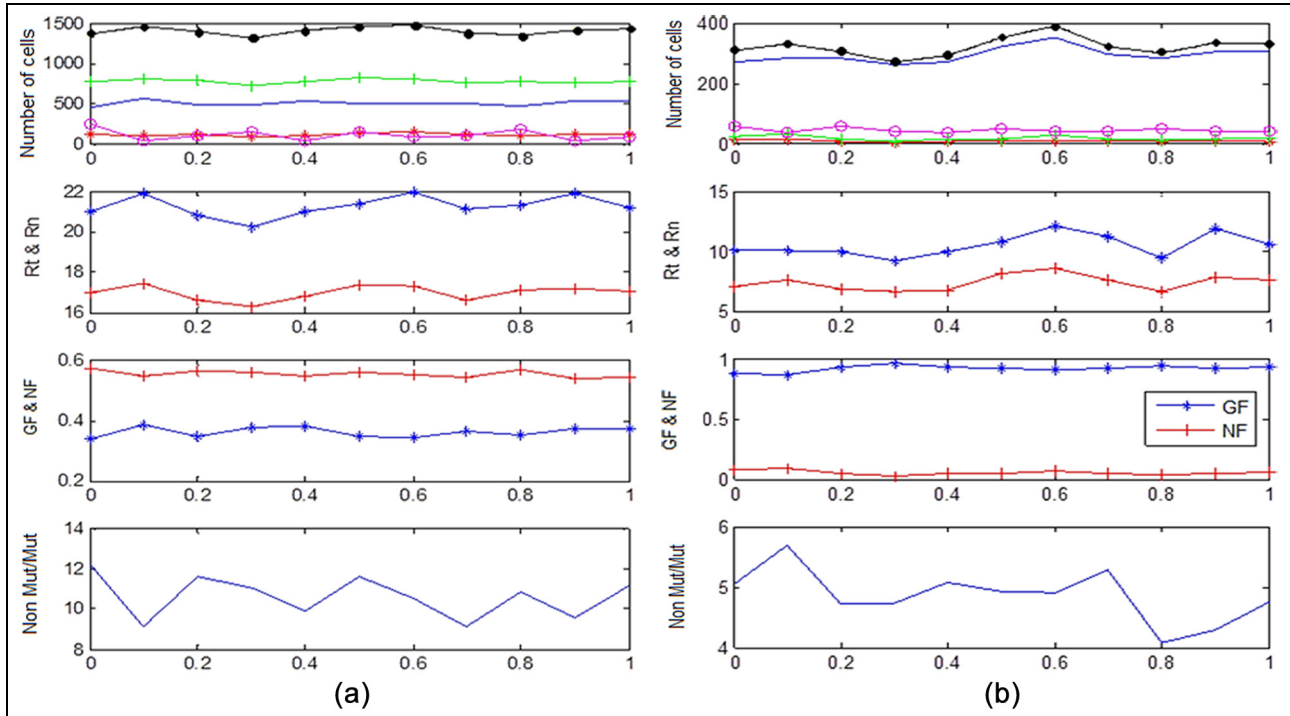


Figure 15. Top to bottom: the number of PT, NT, Ne, T (total tumor), and I cells are shown by the colors blue, red, green, black, and pink (or with symbols -, *, ., +, and o, respectively)—the changes of the radius of the tumor (*blue) and the radius of the necrotic core (red)—the changes of the growth fraction (*blue) and necrotic fraction (red)—the changes of the ratio of the non-mutant PT to mutant PT cells. Changes in N_{mm} and at two arbitrary simulation times: (a) 20; (b) 50. (Color online only.)

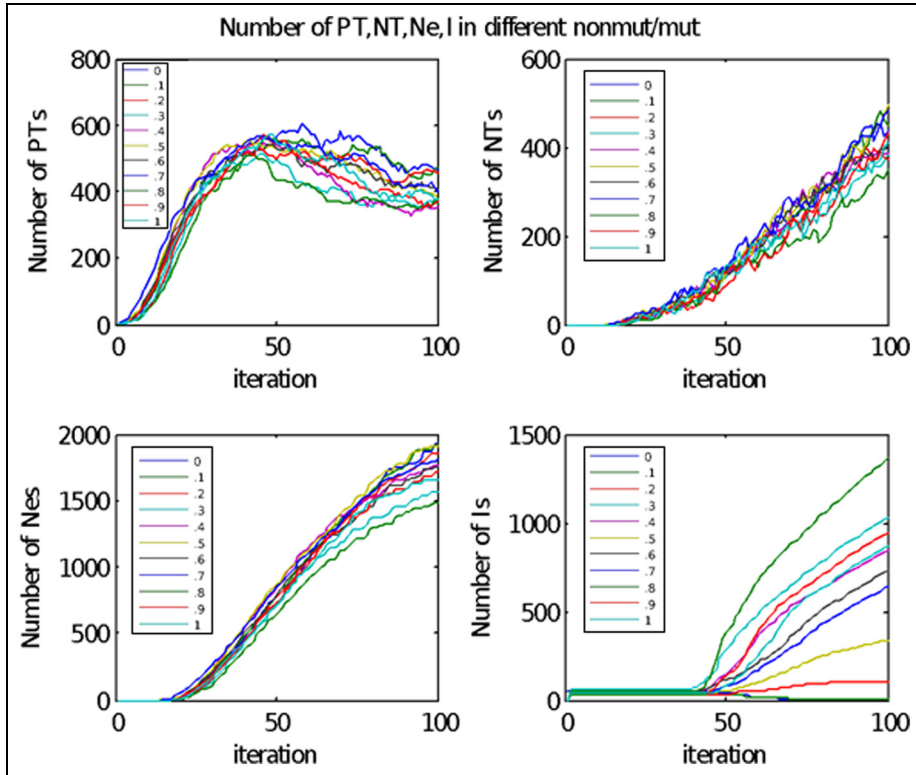


Figure 16. The effect of the variation of K_0 on the number of PT, NT, Ne, and I cells.

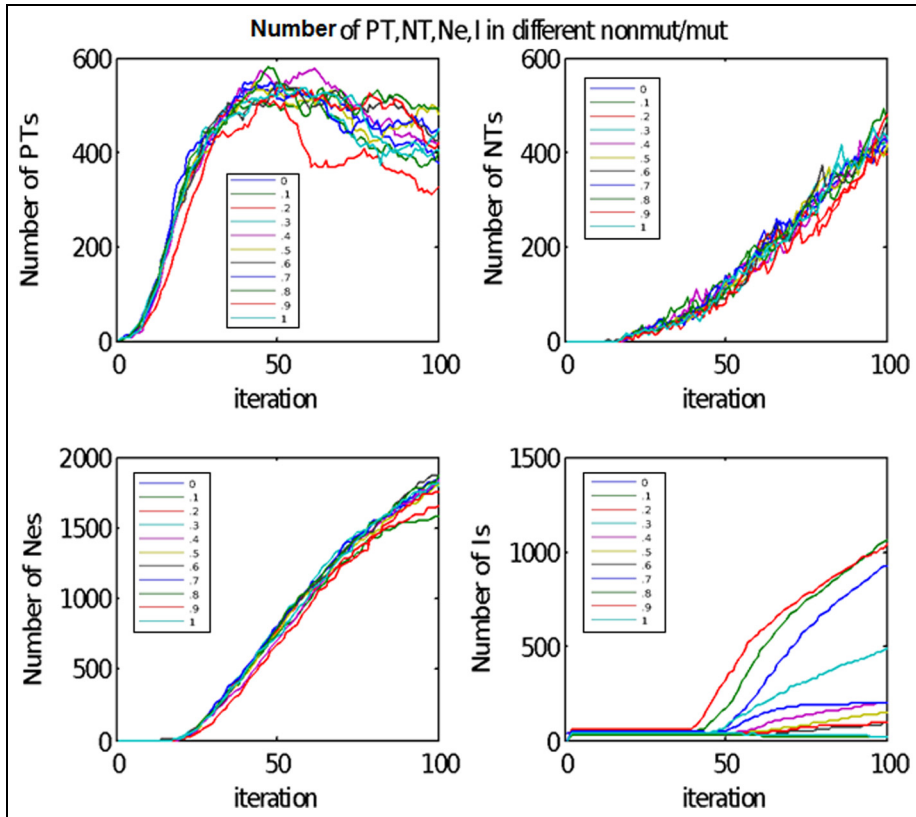


Figure 17. The effect of the variation of K_1 on the number of PT, NT, Ne, and I cells.

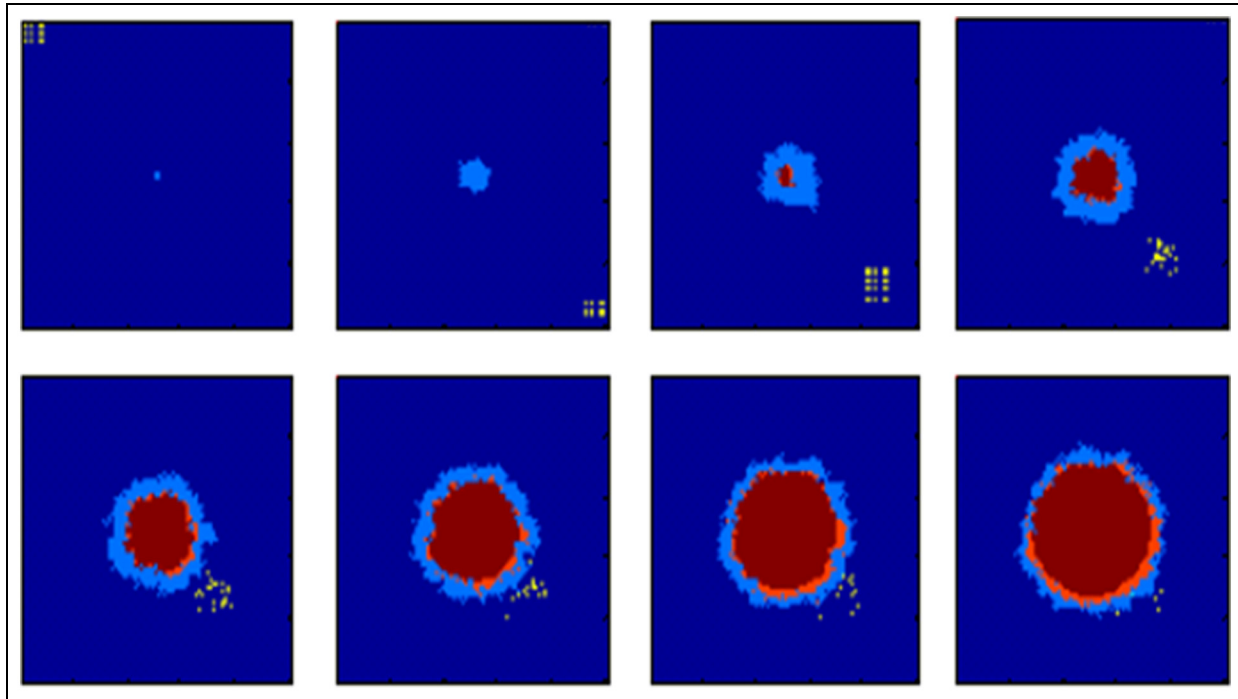


Figure 18. The influx of agent IC from a corner of the lattice and interaction with agent NIC and immune cell recruitment at simulation time $t = 1, 10, 20, 30, 40, 50, 60$, and 80 with the assumption of $KI = 1$. The light-blue (medium gray), light-red (light gray), and dark red (dark gray) regions comprise proliferating cells, non-proliferative cells, and necrotic cells, respectively. The yellow (white) dots are immune cells. The scales are in millimeters.

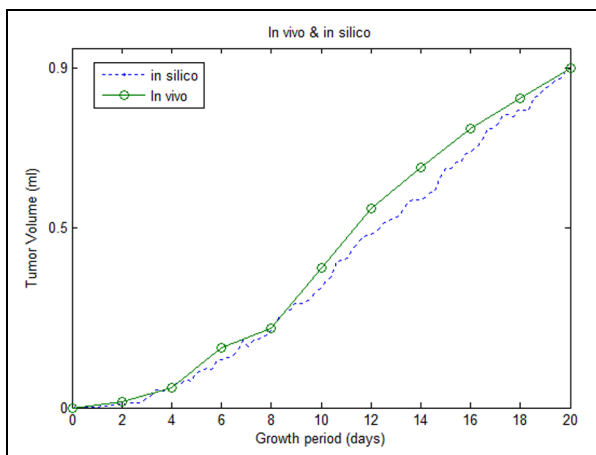


Figure 19. The tumor volume of the developing tumor versus time. The blue dashed line corresponds to the simulation result using the parameters set given in the text. The green plotted circles reflect the in vivo results derived from the medical literature.⁴⁶

quality of the tumor-immune interaction. At small values of Nmm , although some cells of the immune system can recognize cancer cells as abnormal and kill them, the response might not be strong enough to destroy cancer.

Since the immune cells failed to kill tumor cells in this case, no extra immune cell would be recalled in the studied tissue. The tumor grows unlimitedly in tissue regardless of the existence of immune cells, and the number of immune cells in the studied tissue will temporarily decrease. This may show the immune system's deficiency, which may be caused by different microenvironmental factors, for example HIV infection,⁴⁴ leading to increased risk of developing different kinds of cancer.

The effect of hypoxia is also introduced by using Nmm as the initial ratio of the number of non-mutant PT cells to mutant PT cells. Therefore, the lower the Nmm , the more hypoxia effects are shown in our model. On the other hand, it is proven that lower levels of physiological oxygen concentrations or hypoxia affect the HIV-1 transcription and replication.⁴⁵ In fact, this astonishing result of the present model is similar to the results reported in the literature as the first evidence that HIV-1 is inhibited at hypoxia.⁴⁵ Therefore, the proposed model can be extended in order to study the situation in which a patient with HIV infection suffers from cancer in a more realistic way.

Figure 19 shows the volume of the developing tumor in comparison with a set of tumor xenograft experiments.⁴⁶ The tumor volumes are normalized by dividing by the maximum tumor volume at the end of the simulations/experiments for simplicity. The simulations are run using

5-hour time steps. The circles are experimental data collected from male nude BALB/c mice between the ages of 6 and 8 weeks obtained from Vital River Laboratories (VRL; Beijing, China). Tumors were established by the subcutaneous injection of 5×10^6 TFK-1 cells into the flanks of the mice.⁴⁶ The dashed line indicates the result of the present model. Although our results do not give the best fit to the experimental data, they still show the same growth dynamics.

5. Conclusion

One of the significant goals of introducing and implementing a mathematical and computational model is to find new methods for the prevention or treatment of tumors. Studying and predicting phenomena that seem impossible to evaluate in tumor growth or avoiding spending a lot of time and money can be easily done with the help of these models. In the present paper, a new stochastic agent-based model of a solid tumor growth is introduced. The effect of the immune system and tumor-immune interaction are considered. Moreover, the effect of the hypoxia phenomenon that is the low concentration of oxygen in the tumor microenvironment is considered. For considering the effect of the microenvironment and hypoxia, two types of proliferating tumor cells are assumed in the model, namely mutant and non-mutant PT cells. The probability of non-mutant proliferating cells is influenced by environmental conditions, since it is dependent on the number of empty spaces in the Moore neighborhood. In fact, the smaller the number of cells in the neighborhood of a cell, the smaller the consumption of the oxygen and, therefore, the more likely the division of these cells is.

Compelling evidence suggests that immune cells play an important role in the control of malignancy.⁴⁷ Therefore, entering the effect of the immune system adds more physiological details to the model. Considering the novel entrance of the immune cells to the studied tissue, their special movement toward the necrotic core, and the recruitment of immune cells are some novelties of the proposed model. Immune cells appear in the tissue immediately after receiving signals from the tumor cells. In this case, the immune cells move toward the source of signal transmitters, which have been growing considerably so far. When the proportion of proliferating tumor cells to necrotic cells reaches a certain value, the immune cells move randomly to seek tumor cells. Finally, the immune cells may die with a specific probability when they meet tumor cells. The recruiting of immune cells is another assumption proposed in this model. In fact, the more successful are the immune cells in killing the tumor cells and the less failure they face, the more they enter into the tissue to contribute to the destruction of tumor growth.

The discrete nature of the model enables us to simulate complex situations directly with only small changes in the

physiological parameters of the model. The model can easily be extended or modified as new data becomes available or when different situations arise requiring the changes in cell behavior rules. In addition, the presence of the immune system that leads to early detection of tumor growth and the immune cell recruitment for surpassing foreign agents are the features of this model. Although, by taking a superficial glance at our model, one may conclude it shows the same results as some previous models, our model is more compatible with biological facts, since it can show the failure of the immune system, which may happen for example by HIV infection, which leads to a higher risk for developing several types of cancer. Besides, our results show the effect of the microenvironment on tumor growth and on the rest of the system, especially the immune system. In fact, the effect of hypoxia is modeled by introducing two different types of PT cells, and the N_{mm} -parameter as the initial ratio of the number of non-mutant to mutant PT cells. One of the outcomes of our model is that our results confirm the first evidence that HIV-1 is inhibited at hypoxia. Therefore, by extending the present model, we can study HIV-infected patients with concurrent cancer in a more realistic way.

Immune therapy—using the body's own immune system to fight cancer—is an effective cancer treatment. Hence, adding the effects of the immune system to the present model can significantly help better understand the immune therapy in future studies. In addition, the model can be developed to study metastasis, which is a very important phenomenon in malignant tumors. The development of the model to study the effects of therapy on the tumor growth is the authors' future goal. In addition, considering that the immune system may help the tumor grow rather than having anti-tumor effects can also help us improve the recruitment process. Therefore, the results of the model will be more realistic compared to physiological findings.

Acknowledgment

The authors are grateful for the valuable comments and suggestions from the respected reviewers. Their valuable comments and suggestions have enhanced the strength and significance of our paper.

Funding

This research received no specific grant from any funding agency in the public, commercial, or not-for-profit sectors.

References

- Deisboeck TS, Zhang L, Yoon J, et al. In silico cancer modeling: is it ready for prime time? *Nat Clin Pract Oncol* 2009; 6: 34–42.
- Roose T, Chapman SJ and Maini PK. Mathematical models of avascular tumor growth. *Siam Rev* 2007; 49: 179–208.

3. Bast RC, Kufe DW, Pollock RE, et al. *Cancer medicine*. Hamilton, Ontario: BC Decker. Inc., 2000.
4. Materi W and Wishart DS. Computational systems biology in cancer: modeling methods and applications. *Gene Regul Syst Bio* 2007; 1: 91–110.
5. Hanahan D and Weinberg R A. The hallmarks of cancer. *Cell* 2000; 100: 57–70.
6. Hoga CS, Murray BT and Sethian JA. Simulating complex tumor dynamics from avascular to vascular growth using a general level-set method. *J Math Biol* 2006; 53: 86–134.
7. Hanin L. Why victory in the war on cancer remains elusive: biomedical hypotheses and mathematical models. *Cancers* 2011; 3: 340–367.
8. Durrett R. Cancer modeling: a personal perspective. *Not AMS* 2013; 60: 304–309.
9. Torquato S. Toward an Ising model of cancer and beyond. *Phys Biol* 2011; 8: 015017–015039.
10. Bazghandi A. Techniques, advantages and problems of agent based modeling for traffic simulation. *Int J Comput Sci* 2012; 9: 115–119.
11. Deisboeck TS, Wang Z, Macklin P, et al. Multiscale cancer modeling. *Ann Rev Biomed Eng* 2011; 13: 127–155.
12. Wang Z, Butner JD, Kerketta R, et al. Simulating cancer growth with multiscale agent-based modeling. *Seminars in Cancer Biology* 2015; 30: 70–78. Academic Press.
13. Mallet DG and De Pillis LG. A cellular automata model of tumor–immune system interactions. *J Theor Biol* 2006; 239: 334–350.
14. Burkholder B, Huang RY, Burgess R, et al. Tumor-induced perturbations of cytokines and immune cell networks. *BBA Rev Can* 2014; 1845: 182–201.
15. Chew V, Toh HC and Abastado JP. Immune microenvironment in tumor progression: characteristics and challenges for therapy. *J Oncol* 2012; 2012: 1–10.
16. Grivennikov SI, Greten FR and Karin M. Immunity, inflammation, and cancer. *Cell* 2010; 140: 883–899.
17. Janeway CA, Travers P, Walport MJ, et al. *Immunobiology: the immune system in health and disease*. London: Churchill Livingstone, 2001.
18. Burton AC. Rate of growth of solid tumours as a problem of diffusion. *Growth* 1966; 30: 159–176.
19. Kansal AR, Torquato S, Harsh GR, et al. Simulated brain tumour growth dynamics using a three-dimensional cellular automaton. *J Theor Biol* 2000; 203: 367–382.
20. Abbott R. *CancerSim: a computer-based simulation of Hanahan and Weinberg's Hallmarks of Cancer*. Doctoral Dissertation, The University of New Mexico, 2002.
21. Hanahan D and Weinberg RA. The hallmarks of cancer. *Cell* 2000; 100: 57–70.
22. Moreira J and Deutsch A. Cellular automaton models of tumor development: a critical review. *Adv Complex Syst* 2002; 5: 247–267.
23. Ferreira A, Lipowska D and Lipowski A. Statistical mechanics model of angiogenic tumor growth. *Phys Rev E* 2012; 85: 010901.
24. Peirce SM. Computational and mathematical modeling of angiogenesis. *Microcirculation* 2008; 15: 739–751.
25. Scianna M, Bell C and Preziosi L. A review of mathematical models for the formation of vascular networks. *J Theor Biol* 2013; 333: 174–209.
26. Williamson M. Mathematical models of invasion. In: Drake JA, Mooney HA, di Castri F, et al. (eds) *Biological invasions: a global perspective*. Chichester: John Wiley and Sons, 1989, pp.329–350.
27. Vaupel P, Kallinowski F and Okunieff P. blood flow, oxygen and nutrient supply, and metabolic microenvironment of human tumors: a review. *Cancer Res* 1989; 49: 6449–6465.
28. Ungefroren H, Sebens S, Seidl D, et al. Interaction of tumor cells with the microenvironment. *Cell Commun Signal* 2011; 9: 992–1009.
29. Nicola B and Luigi P. multiscale modeling and mathematical problems related to tumor evolution and medical therapy. *Comput Math Methods Med* 1990; 5: 111–136.
30. Araujo RP and McElwain DLS. A history of the study of solid tumour growth: the contribution of mathematical modelling. *Bull Math Biol* 2004; 66: 1039–1091.
31. Byrne HM, Alarcon T, Owen MR, et al. Modeling aspects of cancer dynamics: a review. *Philos Trans A Math Phys Eng Sci* 2006; 364: 1563–1578.
32. Chaplain M. Modelling aspects of cancer growth: insight from mathematical and numerical analysis and computational simulation. In: *Lecture notes in mathematics: Vol. 1940. Multiscale problems in the life sciences*. Berlin: Springer, 2008, pp.147–200.
33. Hatzikirou H, Breier G and Deutsch A. Cellular automaton models for tumor invasion. In: Meyers RA (ed.) *Encyclopedia of complexity and systems science*. Berlin Heidelberg: Springer, 2008, pp. 1–13.
34. Rejniak KA and Anderson ARA. Hybrid models of tumor growth. *Wiley Interdiscip Rev Syst Biol Med* 2011; 3: 115–125.
35. Merrill SJ. Foundations of the use of enzyme kinetic analogy in cell-mediated cytotoxicity. *Math Biosci* 1982; 62: 219–236.
36. Eikenberry S, Thalhauser C, Kuang Y, et al. tumor-immune interaction, surgical treatment, and cancer recurrence in a mathematical model of melanoma. *PLOS Comput Biol* 2009; 5: e1000362.
37. Wilkie KP and Hahnfeldt P. modeling the dichotomy of the immune response to cancer: cytotoxic effects and tumor-promoting inflammation. *arXiv (q-bio.CB)* 2013; 1305: 3634–3658.
38. Yafia R. A study of differential equation modeling malignant tumor cells in competition with immune system. *Int J Biomath* 2011; 4: 185–206.
39. Adam JA and Bellomo N. *A survey of models of tumor–immune system dynamics. Modeling and simulation in science, engineering and technology*. Basel: Birkhäuser, 1997.
40. Wilkie KP. A review of mathematical models of cancer–immune interactions in the context of tumor dormancy. In: Enderling H, et al. (eds) *Systems biology of tumor dormancy. Advances in experimental medicine and biology* 734. New York: Springer, 2013, pp.201–234.
41. Eftimie R, Bramson JL and Earn DJD. Interactions between the immune system and cancer: a brief review of non-spatial mathematical models. *Bull Math Biol* 2011; 73: 2–32.

42. Olsen MM and Siegelmann HT. Multiscale agent-based model of tumor angiogenesis. *Proc Comput Sci* 2013; 18: 1016–1025.
43. Shankaran V, Ikeda H, Bruce AT, et al. IFN γ and lymphocytes prevent primary tumour development and shape tumour immunogenicity. *Nature* 2001; 410: 1107–1111.
44. Corthay A. Does the immune system naturally protect against cancer? *Front Immunol* 2014; 12: 197.
45. Charles S, Ammosova T, Cardenas J, et al. Regulation of HIV-1 transcription at 3% versus 21% oxygen concentration. *J Cell Physiol* 2009; 221: 469–479.
46. Li S, Han Z, Ma Y, et al. Hydroxytyrosol inhibits cholangiocarcinoma tumor growth: an in vivo and in vitro study. *Oncol Rep* 2014; 31: 145–152.
47. Blattman JN and Greeberg PD. Cancer immunotherapy: a treatment for the masses. *Science* 2004; 205: 200–205.

Author biographies

Fateme Pourhasanzade is a PhD candidate in Biomedical Engineering at the School of Electrical

Engineering, Iran University of Science and Technology (IUST), Tehran, Iran.

SH Sabzpooshan is an assistant professor at the Iran University of Science and Technology (IUST). He is with the Department of Biomedical Engineering and the research laboratory of biomedical signals and sensors, IUST, Tehran, Iran.

Ali Mohammad Alizadeh is an assistant professor at the Tehran University of Medical Sciences (TUMS), and is the founder of (Pre) Clinical Cancer Research Group (PCCRG). For more details you can visit www.pccrg.org.

Ebrahim Esmati is an assistant professor at the Tehran University of Medical Sciences, Department of Radiation Oncology, Cancer Institute, Tehran, Iran.